

Urban microclimate prediction based on weather station data and artificial neural network



Senwen Yang^a, Dongxue Zhan^a, Theodore Stathopoulos^a, Jiwei Zou^a, Chang Shu^b, Liangzhu Leon Wang^{a,*}

^a Centre for Zero Energy Building Studies, Department of Building, Civil and Environmental Engineering, Concordia University, Montreal H3G 1M8, Canada

^b Construction Research Centre, National Research Council Canada, Canada

ARTICLE INFO

Keywords:

Urban microclimate
Urban heat island (UHI)
Field measurements
Building energy consumption
Machine learning
Artificial neural network

ABSTRACT

Urban microclimate has a significant impact on building energy consumption. Building energy modeling (BEM) requires accurate local weather conditions near a target building, whereas Typical Meteorological Year (TMY) weather inputs often use remote airport weather data. An artificial neural network (ANN) model is presented in this study to predict urban microclimates based on long-term measurements from local weather stations near urban buildings and their significance in analyzing building energy consumption. By utilizing only a few months of data, the ANN model could connect local and remote meteorological parameters for a whole year. The 20-year historical weather data at the airport was then used to generate a local TMY. Based on the original and local TMYs, this study compared building heating and cooling loads. This method was evaluated for five weather stations within the city of Montreal to assess the impact of the local microclimate on the energy consumption of buildings. Based on locations, urban microclimate contributed to an additional 2 % to 14 % cooling energy consumption and a reduction of 1 % to 10 % winter heating energy consumption.

1. Introduction

In the last decades, cities have faced significant challenges from rapid urbanization, mounting energy consumption, and increasing impacts of climate change, such as more heatwaves and other weather extremes [1,2]. By 2050, over 70 % of the global population is estimated to live in urban areas [3]. There is an increasing need for energy to support the growing population and better living environments. Many of these human activities and their interactions with climate change occur inside the region of urban microclimate [4–6]. Urban microclimate refers to the immediate surrounding environment (vertical and horizontal) around building clusters inside the urban boundary layer with a height of 2 ~ 5 times the average building, including any climatic phenomenon of urban physics. Urban geometry was found to be an important factor affecting the urban microclimate [7–9]. In particular, local meteorological conditions near a building are the primary determinants of

thermal exchanges through building envelopes in temporal and spatial resolutions [9,10]. Previous studies reveal the correlation between urban geometry characteristics and urban microclimate for a specific city region [11,12]. The urban configurations are also demonstrated to contribute to urban heat islands in various cities [13–15]. The situation can be elevated during extreme weather. For example, a recent study by Hong et al. [16] showed up to 11 °C outdoor air temperature differences between the coastal and downtown areas in San Francisco during the record 2017 heatwave. Therefore, accurately estimating urban microclimate conditions is imperative for a better prediction of building energy consumption, especially in the context of climate change and increasing weather extremes.

Extensive research has consistently shown the crucial role of urban microclimate in building energy consumption [17,18]. Heat and mass exchanges between buildings and their surrounding environment significantly contribute to energy loads. Previous reviews summarize

Abbreviations: ANN, Artificial Neural Network; BEM, Building Energy Model; BES, Building Energy Simulation; CFD, Computational Fluid Dynamics; DOE, U.S. Department of Energy; LSTM, Long Short-Term Memory; MAE, Mean Absolute Error; MAPE, Mean Absolute Percentage Error; ML, Machine Learning; MLP, Multiple Layer Perceptron; MLR, Multiple Linear Regression; NLR, Nonlinear Regression; R², Correlation Coefficient; RF, Random Forest; RMSE, Root Mean Square Error; SHGC, Solar Heat Gain Coefficient; SRC, Standardized Regression Coefficient; SVI, Sensitivity Value Index; TMM, Typical Meteorological Month; TMY, Typical Meteorological Year; UHI, Urban Heat Island; VAV, Variable Air Volume.

* Corresponding author.

E-mail address: leon.wang@concordia.ca (L.L. Wang).

<https://doi.org/10.1016/j.enbuild.2024.114283>

Received 1 February 2024; Received in revised form 2 May 2024; Accepted 11 May 2024

Available online 13 May 2024

0378-7788/© 2024 The Author(s). Published by Elsevier B.V. This is an open access article under the CC BY-NC-ND license (<http://creativecommons.org/licenses/by-nc-nd/4.0/>).

that urban microclimate could lead to a median rise of 19 % in cooling energy usage and a median reduction of 19 % in heating energy usage [19]. The impact varied in different cities, and cooling energy consumption increased ranging from 10 % to 120 %, and conversely, heating energy consumption decreased ranging from 3 % to 45 %. Another study [20] showed that daily temperature rise increased electrical energy consumption typically by 2.6 % during a summer day. The spatial difference of urban microclimate impact, as mostly manifested by urban heat island (UHI) intensity, was found to peak at the urban center and showed a decreasing urban–rural trend. It was indicated by another study [21] that the UHI can contribute to 15 % to 200 % cooling energy consumption increase.

The prediction of urban microclimate conditions for the purpose of building energy modeling has been challenging. A previous review [22] shows that most approaches used to develop building energy models neglect the UHI effect in neighborhoods. Instead, they rely on climate data from meteorological weather stations in more distant rural areas [23]. A few studies applied Urban Weather Generator (UWG) to consider the urban microclimate [24–26] and researchers utilized it to analyze its impact on building energy consumption [27]. A few researchers also implemented the PALM-4U model to evaluate the urban microclimate and urban heat island covering multiple parameters by microscale simulation [28–30]. Researchers also implement the CFD approach with building energy consumption (BES) to investigate the impact on building energy performance [20,31]. Recent research highlights that the estimation of building energy usage varies significantly depending on whether the UHI influence on the urban microclimate is considered. However, due to the challenges associated with obtaining accurate temperature data incorporating the UHI effect, only a few studies have explored the interplay between urban microclimate and building energy performance. Most studies nowadays have not taken UHI impact into consideration [32].

The quantification of urban microclimate often relies on four approaches: field measurements and meteorological observations, wind tunnel experiments, CFD simulations, and recent developments in artificial intelligence (AI) and machine learning (ML) approaches [6]. A recent review study has documented AI and ML approaches and a detailed comparison of all the approaches well [6]. Data-driven urban microclimate predictions have progressed well in recent years thanks to advancements in computing power for handling high-dimensional data. One of the first applications may date back to a study in 2016 [33], which categorized the local climate zones with various landscape features, and the number of applications increased in the following years. Artificial intelligence models were applied based on the parameters of interest, including multiple linear regression (MLR) [34,35], nonlinear regression (NLR) [35,36], random forest (RF) [34,35], and artificial neural networks (ANN) [22,23]. For predicting wind speed and wind power, Mortezaee et al. [37] adopted the machine learning method with CFD simulation results to assess the wind power potential in the urban region. According to a recent study by Alonso [34], multiple machine-learning models were developed to investigate the relationship between air temperature and different factors (vegetation, sky view factors, the density of water bodies, buildings, moisture, radiation, etc.), and the results were satisfactory. The performance of this model still needs further confirmation due to the lack of long-term testing data and multiple location testing data. Recently, a recurrent neural network was applied to model the variation in time-series temperature under the urban street canyon. Zhang et al. [38] implemented the long short-term memory (LSTM) model to forecast the wind speed, wind direction, relative humidity, and solar radiation and then applied the predicted weather parameters for building energy estimation. This method shows more reliable energy estimation compared with the use of Typical Meteorological Year (TMY) weather data.

ANN was found to perform well for predictions in the urban microclimate [22,25]. Zhang et al. employed long short-term memory (LSTM) to predict urban microclimate and investigated its influence on

buildings of different shapes [22,25]. Moghanlo et al. [39] utilized an ANN model to predict the impact of climate changes in the Zanjan region of northwest Iran. This study analyzed daily meteorological data from 1988 to 2018, considering observed variables such as maximum and minimum temperature and precipitation as predictors in the ANN. Xie et al. utilized an ANN model to predict the mean radiant temperature surrounding buildings [40]. Guijo-Rubio et al. utilized an artificial neural network (ANN) model with three different neural structures to achieve highly accurate predictions of solar radiation using satellite image data [41]. Shboul et al. employed an ANN model to simultaneously predict hourly solar radiation and wind speed, as did another similar study [42]. These previous studies applied neural network models to predict the outdoor environment and showed acceptable results. However, there are very limited studies using ANN investigating the relationship between the rural metrological weather station and local urban microclimate or urban heat island.

The numerical model required detailed information as boundary conditions to include multiple factors. Meanwhile, to evaluate the energy consumption of buildings, TMY weather data is often used to represent annual typical weather patterns based on the historical data of at least 20 years [43]. Nowadays, numerous datasets in accessible formats are available for various regions globally. However, these datasets originate from reference weather stations often situated outside urban areas, even if they can be different from localized weather conditions [23]. However, obtaining 20 years of localized measurements for urban microclimates in multiple localized regions is often not feasible. Thus, how to rely on limited measurement data to evaluate the urban microclimate and generate long-term localized TMY data remains a research question when investigating the urban microclimate impact on building energy consumption.

There are still many challenges to evaluating the urban microclimate and its impact on building energy consumption. Since there is a lack of efficient methods to evaluate the long-term climatic and local impacts of urban microclimate on building energy performance, previous research focuses on urban microclimate impact on building energy demand for specific periods mostly based on numerical simulation; instead of using actual local measurements such as weather stations. How long-term local weather station measurements can be used to consider future local climatic and urban heat island impacts remains unclear. This is because the relationships between the local, the airport data and the historical and future climate data are often non-linear and site-specific, so the conventional linear regressions may not perform well. Therefore, this study evaluates how ANN can be applied to quantify complex relationships based on detailed onsite weather station measurements with low computational cost. Since a city often has abundant weather station data, the proposed method can be readily applied by other researchers to consider the impacts of local and future climatic impacts on building energy performance.

This study introduces a new approach to investigating the influence of urban microclimates on building energy modeling based on the data-driven method to address the complex non-linearity of the local and rural weather data, and the historical and future climatic data without increasing computational cost and, complex boundary setting, when compared to other numerical models such as UWG, CFD, etc. We employ ANN to establish the connection between our one-year (Year of 2021) measurements of local and airport weather station data. Then, the developed ANN model is applied to generating historical local weather using the 20-year airport weather records. Additionally, using the historical local weather data, this approach yields a “localized” Typical Meteorological Year (TMY). This localized data is then passed into EnergyPlus to evaluate the impact of urban microclimate on building energy consumption.

2. Methodology

The process of this study can be divided into three sections: urban

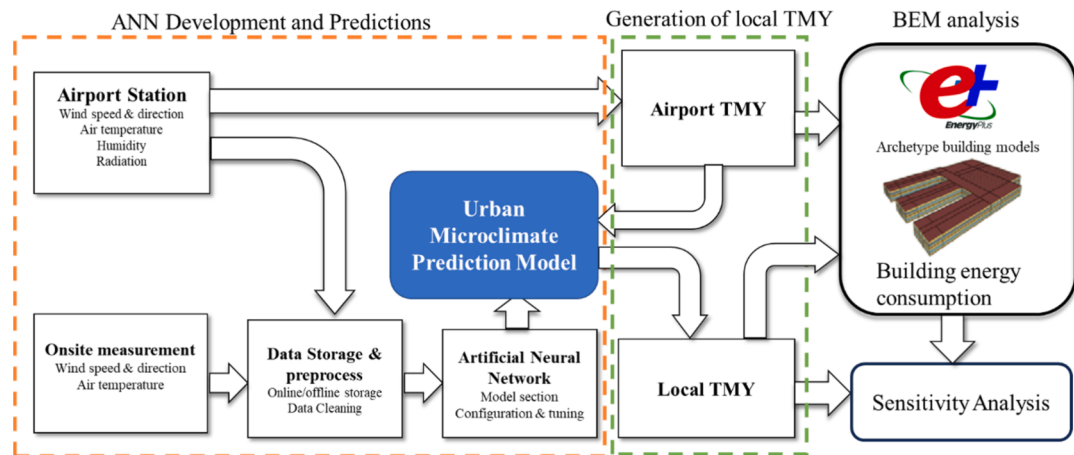


Fig. 1. Overall schematic for using ANN to estimate building energy.

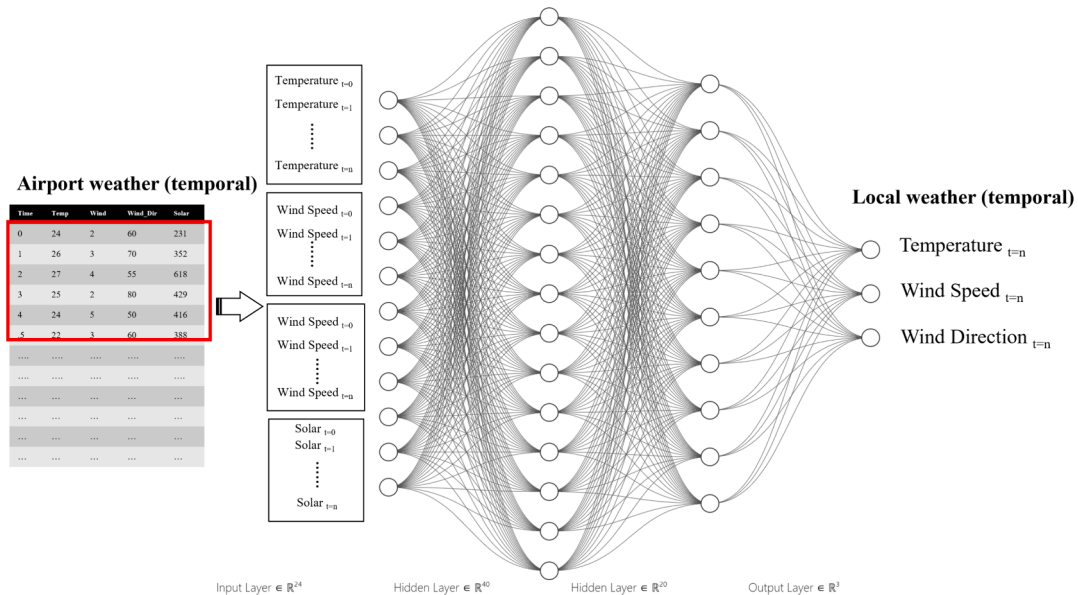


Fig. 2. Structure of proposed ANN model.

microclimate model development and training, local weather prediction and TMY generation, and building energy modeling. As shown in Fig. 1, this study starts with weather data collected from publicly available historical airport datasets and onsite collection by local weather stations. Then, an ANN model was trained and tuned to find the connection between airport weather (which is regarded as undisturbed weather) and local weather (weather under the urban microclimate impact). After obtaining the ANN model, the historical long-term weather data were used to generate the long-term local weather data with urban microclimate information embedded. A local TMY weather file was created by following the established statistics method for the building energy analysis by EnergyPlus [44] of the DOE archetype buildings [45].

2.1. ANN models for urban microclimate

The ANN model has been used in several studies related to urban microclimate [39,40,46,47], which showed that the ANN model can have good performance in urban weather prediction. Moghanlo et al. [39] utilized an ANN model to predict the impact of climate change. Xie et al. [40] developed an ANN model to evaluate the mean radiant temperature surrounding buildings. Zhang et al. [46] evaluate the microclimate impact on urban microclimate via the ANN model. The

ANN model is reported to have good performance compared to other proposed models in solving the problems related to urban microclimate [34,47,48]. Thus, this study applied similar methods as these previous studies to the current topics, which have not been covered in these previous studies. This study starts with an ANN model with multiple layer perceptron (MLP) and its performance was compared to other basic machine learning models such as linear regression, and random forest.

In this study, airport weather conditions were used as input parameters, while the wind speed, wind direction, and air temperature from local weather station were considered as predicted features of urban microclimate, and multiple layer perceptron was used to train the model, as shown in Fig. 2. By tuning the existing model, the optimized ANN structure consists of one input layer with 24 input neurons, two hidden layers with 40 and 20 neurons, respectively, and one output layer with three neurons for wind speed, direction, and temperature. To consider the thermal storage of the urban underlayer, six hourly data lookback is adopted in the model inputs shown in Fig. 2. The Year 2021 measurement data was applied with the training and testing data split of 0.3, so at least three continuous months of hourly weather data were for training, and the rest were used for testing. After tuning the model with different dataset settings, including the training dataset random

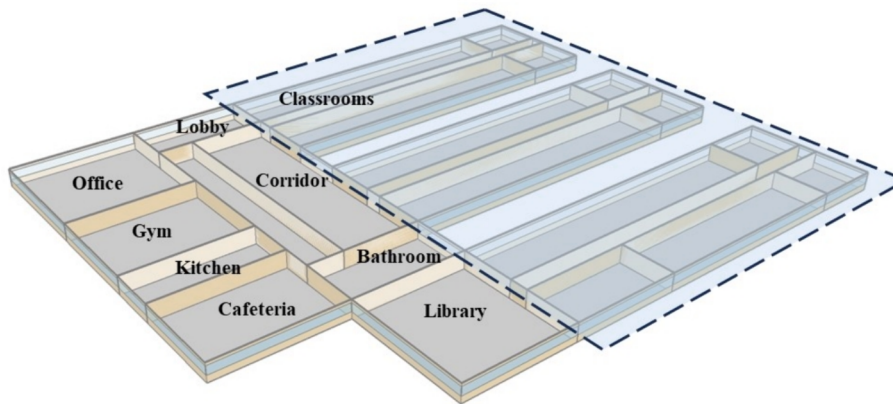


Fig. 3. DOE Building archetype of primary school.

sampling, or continuous data of several months as the training dataset, it was found that the proposed approach would not increase the prediction accuracy anymore when adopting more training data than three months. From the testing with model performance with different dataset settings, the accuracy does no more improve, when training data involves more than 3 months. This approach focuses on how weather parameters affect the temperature and wind difference between the local environment and the airport. During the training and testing, all the parameters are scaled based on the minimum and maximum values. The model performance in extreme weather (heatwave) is highlighted in Figs. 5–7. The performance for the whole year including hot weather and cold weather is evaluated.

As for the input parameters, temporal weather data from the airport are applied as input. The output labels are the local air temperature, wind speed, and wind direction. Meanwhile, the performance of MLP will be compared with basic machine learning models like multiple linear regression [34,35] and random forest [35,37] used in previous urban microclimate studies. Comparing an ANN to a basic model provides a benchmark for evaluating the performance of the ANN. Suppose the ANN does not significantly outperform simpler models such as Linear Regression or Random Forest. In that case, it might indicate that the problem is not complex enough to warrant using ANN. Besides, ANNs are prone to overfitting, especially when the dataset is small or the architecture is too complex. Comparing against simpler models helps gauge whether an ANN truly captures meaningful patterns. This study will also compare the proposed method to the LSTM model used in the previous study [38] to see if a more complicated model is required.

Meanwhile, the accuracy of the model has been tested by calculating the mean absolute error (MAE) in Eq. (1) and the correlation coefficient (R^2) of Eq. (2). Root mean square error (RMSE) in Eq. (3) and mean absolute percentage error (MAPE) of Eq. (4) are also adopted for evaluating wind speed and wind directions.

$$MAE = \frac{\sum_{i=0}^n |y_i - \hat{y}_i|}{n} \quad (1)$$

$$R^2 = 1 - \frac{\sum_{i=1}^n (y_i - \hat{y}_i)^2}{\sum_{i=1}^n (y_i - \bar{y})^2} \quad (2)$$

$$RMSE = \sqrt{\frac{1}{n} \sum_{i=1}^n (y_i - \hat{y}_i)^2} \quad (3)$$

$$MAPE = \frac{1}{n} \sum_{i=1}^n \frac{|y_i - \hat{y}_i|}{y_i} \times 100\% \quad (4)$$

2.2. Local TMY and weather prediction

The evaluation of urban microclimate over a long period of multiple

years adopts the typical meteorological year (TMY) method, a commonly used reference year selection method, to assess climate impacts. The TMY method was developed by selecting 12 months of weather data from a long-term dataset of at least ten years to represent the typical weather conditions for a specified location instead of considering each year inside the selected period. This method avoids the need to consider the impact of the specific yearly climatic variation and reduces significantly the computational cost and repetitive labor work [43,49]. In this study, both the airport and local typical meteorological year (TMY) were generated based on the EN ISO 15927-4 standard [50,51], which is a combination of multiple typical meteorological months (TMM). TMMs are selected by comparing each month's distribution with that month's long-term distribution for the available climate dataset through the Finkelstein–Schafer statistics based on air temperature, global horizontal irradiance, relative humidity, and wind speed. The detailed procedure of TMY generation of this study is shown as follows.

First, for a single climate variable and target calendar month, the cumulative distribution function for the selected-year y , $SY(y, i)$ and whole-years dataset, $WY(y, i)$ are calculated by Eqs. (5) and (6):

$$SY(y, i) = \frac{S(A_i)}{n + 1} \quad (5)$$

$$WY(y, i) = \frac{W(A_i)}{N + 1} \quad (6)$$

where, i is the calendar day of the calendar month, A_i is the daily mean of the selected climate variable at day i , $S(A_i)$ is the rank order of A_i within the calendar month of the selected-year dataset, n is the number of days in the calendar month, $W(A_i)$ is the rank order of A_i within the calendar month of the whole-year dataset, N is the number of days in the calendar month in the whole-year dataset.

With $SY(i)$ and $WY(i)$ in the above equations, the Finkelstein–Schafer statistic for each calendar month could be calculated:

$$Fs(y) = \sum_{i=1}^n |SY(y, i) - WY(y, i)| \quad (7)$$

For each climate variable and each calendar month, the rank score is evaluated for each year inside the whole-year dataset based on the $Fs(y)$ value. Repeat the above procedures for parameters including air temperature, relative humidity, global horizontal irradiance, etc., and then calculate the sum of $Fs(y)$.

2.3. Building energy model and sensitivity analysis

2.3.1. Building energy model

The reference building energy model (BEM) for a primary school

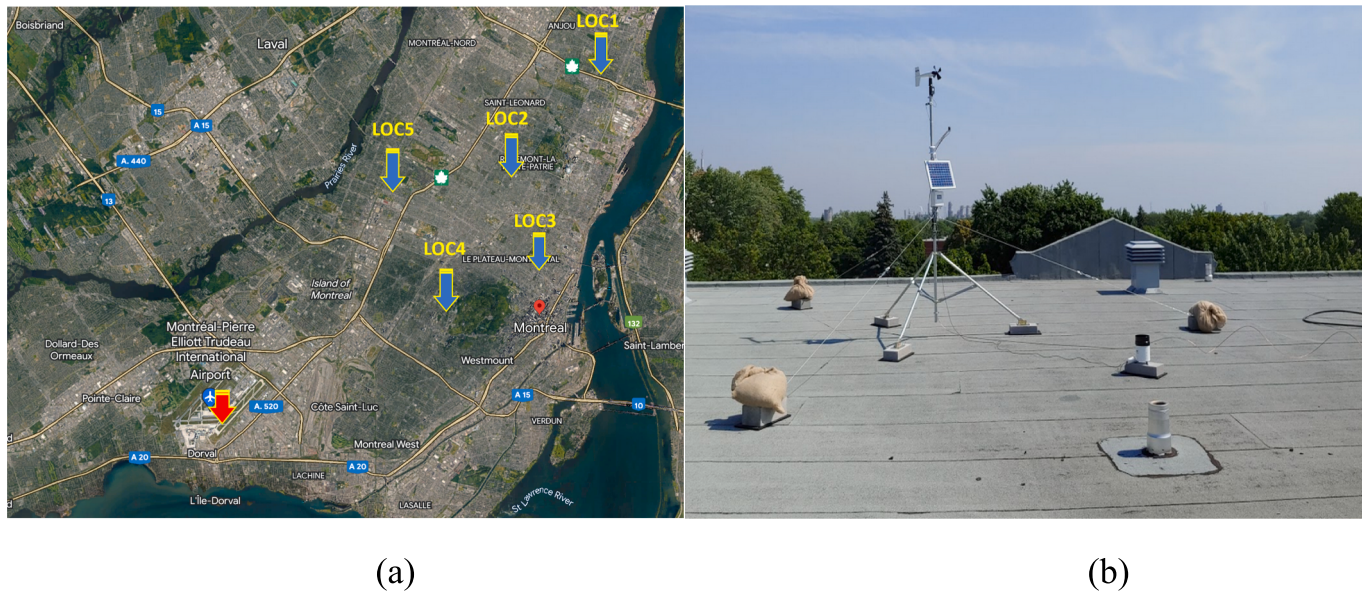


Fig. 4. (a) Location and installation of roof-mounted weather stations (b) weather station sensors and configuration and installation in LOC1.

building was chosen as the case study for Climate Zone 6A, the Cold-Humid Climate. The reference model was developed by the U.S. Department of Energy (DOE) [52], and in this study, the location of the building is Montreal, Quebec, Canada. The primary school building comprises classrooms, a multipurpose room, a cafeteria, and a kitchen with a main corridor and three classroom zones, as shown in Fig. 3. A table in Appendix A provides various features and descriptions of the building. Specifically, it is a single-story structure with a Gross Floor Area of 6900 m² (approximately 74,000 ft²) equipped with a Variable Air Volume (VAV) system for 25 zones. The floor-to-ceiling height is 4 m, and the window-to-wall ratio is 35 %. The building properties are defined with the U-factors for the roof of 0.18 W/(m²K), external walls of 0.31 W/(m²K), and windows of 2.65 W/(m²K) with a Solar Heat Gain Coefficient (SHGC) of 0.43. The infiltration rate is 0.46 m³ per m² floor area (1.5 ft³/ft²). The heating setpoint is maintained at 21°C from 6:00 AM to 9:00 PM and 16 °C at other times, while the cooling setpoint is 24 °C during operational hours and 27 °C during non-operational hours. The building occupancy density varies across different spaces, with classrooms allowing 4 m²/person, corridors 10 m²/person, and offices 20 m²/person. In the building energy simulation, there are several assumptions for analysis of the impact of urban microclimate. The main parameters considered in this study are air temperature, wind speed, and wind direction. Solar radiation was assumed to be the same as in the airport since the local weather station is installed at the top of the building roof. Additionally, the shading effect of the surrounding buildings is not covered in this study.

2.3.2. Sensitivity analysis

To determine the significance of meteorological parameters, a sensitivity analysis (SA) is applied to evaluate the impact of meteorological parameters on the energy performance of buildings by using the Sensitivity Value Index (SVI) method. This method combines three sensitivity techniques: the Standardized Regression Coefficient (SRC), Random Forest Variable Importance, and T-value analysis [53]. The SRC method relies on regression and is commonly used in building energy assessment. A higher SRC value indicates greater importance of the variable. The Random Forest Variable Importance measures how a model's accuracy is affected by including or excluding a variable, indicating its contribution to output values. The T-value assesses whether the coefficient of a corresponding variable is statistically different from zero. A higher absolute T-value suggests a greater importance of the

variable [54]. SRC and T-value are suitable for linear models. The SVI method, as represented by Eq. (8) [55], comprehensively evaluates the contribution levels of input parameters, and the sensitivity analyses' results were normalized and combined. This approach ensures a more consistent and aggregated assessment of parameter significance. The candidate meteorological parameters in this study are air temperature, wind velocity, wind direction, relative humidity (RH), diffuse solar radiation, normal solar radiation, and global solar radiation.

$$\text{Sensitivity Value Index (SVI)}(\%) = \sum_{l=1}^m \frac{k}{m \bullet k} \times 100 \quad (8)$$

where V is the value of a sensitivity analysis method, i is a parameter, n is the total number of the parameters ($n = 7$), j is a sensitivity method, k is the total number of sensitivity methods ($k = 3$: SRC, random forest variable importance, and T-value), l is the target output, and m is the total number of target outputs ($m = 1$: building energy consumption load, repeated for three times for winter, summer and total).

2.4. Field measurement and data collection

According to Fig. 4(a), the study investigated five weather station locations labeled LOC1, LOC2, LOC3, LOC4, and LOC5. A logger with an LCD screen and cellular communication capability is used by the weather stations. The chosen weather station (refer to Fig. 4(b)) consists of various sensors, such as a temperature and humidity sensor (S-TBH-M002), pyrometer (S-LIB-M003), wind speed sensor (RM Young Wind Monitor Sensor), wind direction sensor (RM Young Wind Monitor Sensor), and rainfall sensor (S-RGB-M002). A detailed description of these sensors can be found in Appendix B. These sensors generally measure temperature, wind speed, and wind direction in specific ranges and conditions. It provides a resolution of 0.02 °C at 25 °C and a temperature accuracy of 0.21 °C between 0 °C and 50 °C. A wind speed range of 0 m/s to 76 m/s can be measured with an accuracy of 1 %. The wind direction sensor covers a range of 0° to 355° with a 5° dead band and has an accuracy of ±5°. The installation area was chosen clear of obstructions, HVAC equipment, and exhaust fans to avoid interference with the sensors. Positioning the tripod away from the roof's edge during installation is important to ensure safety. This minimizes the impact of turbulence caused by the roof's edge on wind speed and

Table 1

Machine learning model performance of temperature predictions.

	MLR	RF	LSTM	ANN(MLP)
R ²	0.97	0.96	0.99	0.996
MAE	0.92	0.88	0.68	0.52
RMSE	1.22	1.01	0.85	0.68

direction sensors. Using concrete anchor bolts, the feet of the weather station tripod are attached to 12 kg concrete blocks. To protect the roof, the tripod's feet and blocks should be placed on rubber mats, while its legs should remain as level as possible. A total of three guy wires, each 4 m long, are used to secure the tripods. More than 50 kg of weight is connected to these wires to secure the installation. For the wind monitor to be placed 3 m above the roof, the tripod mast is vertically leveled using a bidirectional post level. Detailed experimental information about the installation process of the weather stations can be found in the previous study [56].

3. Results and discussion

3.1. ANN development and predictions

3.1.1. Temperature prediction

Table 1 compares the performance based on the coefficient of determination (R^2), Mean Absolute Error (MAE), and Root Mean Square Error (RMSE). Compared to the MLR and RF models, the proposed MLP model performs better. Air temperature prediction using the MLP model has an MAE of 0.52 and RMSE of 0.68 degrees, with an R^2 of 0.996. Compared to the literature [19,25], it shows acceptable results. Existing MLP methods still perform better when predicting air temperatures than LSTM methods. Complex neural network models such as LSTM may have worse performance than basic MLP models when solving simple physical problems.

Fig. 5 shows the air temperature comparison between the measurement data and model prediction results for LOC1 in the testing dataset. **Fig. 5(a)** presents four training models for predicting the air temperature. The four models can capture the trend of temperature temporal variation during the five continuous summer days. Among them, the ANN model has the most accurate prediction. **Fig. 5(b)** compares the predicted and measured temperature testing datasets. The prediction

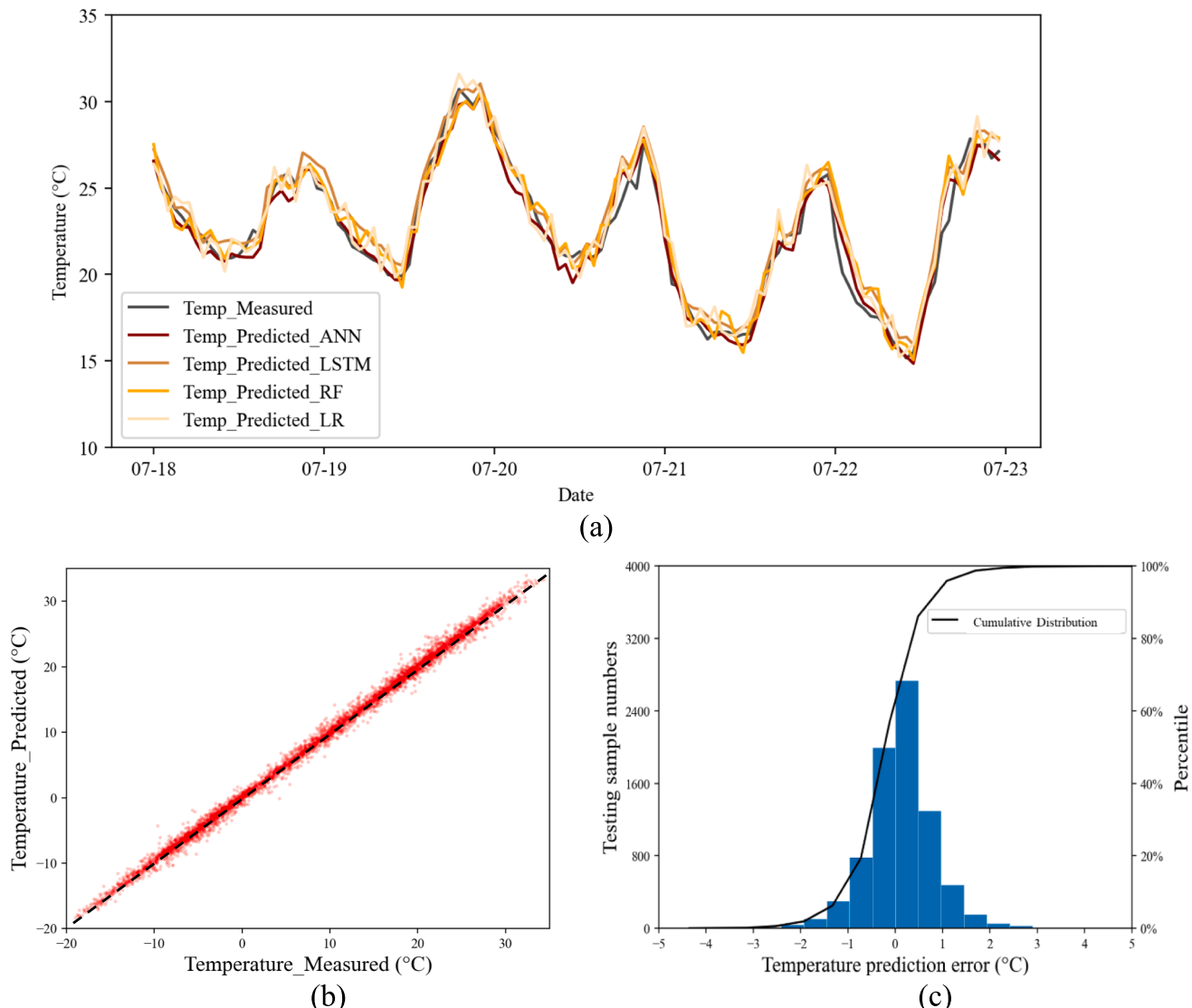


Fig. 5. (a) Air temperature comparison between prediction and measurement from July 18th to 23rd (b) Air temperature prediction accuracy in the testing dataset. (c) Air temperature error distribution at LOC1.

Table 2
ANN model performance at multiple locations.

	R ²	MAE	RMSE	MAPE
LOC1	0.996	0.52	0.68	3.15 %
LOC2	0.994	0.54	0.71	3.21 %
LOC3	0.995	0.53	0.69	3.08 %
LOC4	0.992	0.59	0.8	4.01 %
LOC5	0.994	0.55	0.72	3.65 %

shows good agreement with the measurement data. The error between the measurement and prediction is located ranging from -0.5°C to 0.5°C , meanwhile, the sensor measurement accuracy is around 0.2°C . In this study, 5 locations are investigated. The temperature prediction performance is presented in Table 2. All the locations and models can achieve R² for more than 0.99 and MAE around 0.5°C . It illustrates that the proposed method for predicting air temperature can be applied to different locations. It should be noted that the trained model may be limited to predicting at its own sites, and the model may need to be retrained for another location. Similar results for other locations are presented in Appendix C.

3.1.2. Wind speed prediction

Fig. 6(a) shows the effect of urban microclimate on wind speed in LOC1. Between July 18th and July 23rd, the predicted wind speed was consistent with the measured wind speed. Wind prediction is also found to be close to the estimation based on the wind power-law profile with urban exposure calculated from airport wind speed [57].

$$\frac{V_z}{V_{z_g}} = \left(\frac{Z}{Z_g}\right)^{\alpha} \quad (9)$$

Where Z_g is the gradient height, V_{zg} is the velocity at gradient height, and α is the roughness exponent. Z_g and α are functions of ground roughness. α values for all positions are presented in Table 3.

According to Fig. 6(b), the prediction errors range from -0.4 m/s to 0.6 m/s , which is acceptable for urban microclimate prediction [34,38]. Wind speed prediction and power law calculation compared with measured true data and it shows that the wind speed can have an accuracy of around 0.5 m/s . Considering the wind sensor has an accuracy of around 1.1 m/s , close to the previous study [58], the performance of wind speed prediction might be improved if higher accuracy wind data can be achieved.

Table 3 shows the wind speed prediction performance for all 5 locations. The overall R² for all locations ranges from 0.5 to 0.6, and the

MAE is around 0.5 m/s . It is more challenging to predict wind speed accurately than air temperature because of turbulence and magnitude fluctuation. Another potential reason could be the wind speed measurement accuracy [38]. Data quality and model performance may be improved by using more precise sensors. ANNs are also more accurate at most locations than power law estimations based on roughness calculations. However, based on the R² of wind speed prediction, there is still room to improve the ANN model.

3.1.3. Wind direction prediction

Fig. 7 shows the performance of the wind direction prediction in LOC1. For the North, wind direction is "0", and wind direction in degree increases counterclockwise. From Fig. 7(a), there is good agreement between measured results and predicted results for the hourly wind direction. According to Fig. 7(b), the overall wind frequency in both magnitude and direction in LOC1 shows a good match for the wind's direction and magnitude. Most of the wind comes from the west direction, 225 to 325. According to Fig. 7(c), most wind direction errors fall between 0 and 36 degrees. Similarly, prediction results for other locations are presented in Appendix C.

In Table 4, the wind direction prediction performance is presented for all five locations. Predicted urban MAE, RMSE, and MAPE calculations are presented for wind direction. Overall, LOC3 appears to have the most accurate predictions with the lowest errors, while LOC5 has the least accurate predictions with higher errors. The MAE, RMSE, and MAPE values provide insights into the accuracy and performance of the model at each location. All 5 locations have an MAE close to 30 and an RMSE close to 40 for wind direction, which can be regarded as satisfactory results compared to the previous machine learning studies [38].

Table 3
Wind speed performance and error in all five locations.

	ANN		Power Law		
	R ²	MAE (m/s)	α	R ²	MAE (m/s)
LOC1	0.67	0.55	0.25	0.61	0.62
LOC2	0.62	0.62	0.35	0.65	0.58
LOC3	0.66	0.52	0.35	0.68	0.55
LOC4	0.56	0.81	0.35	0.53	1.04
LOC5	0.52	0.87	0.3	0.49	0.92

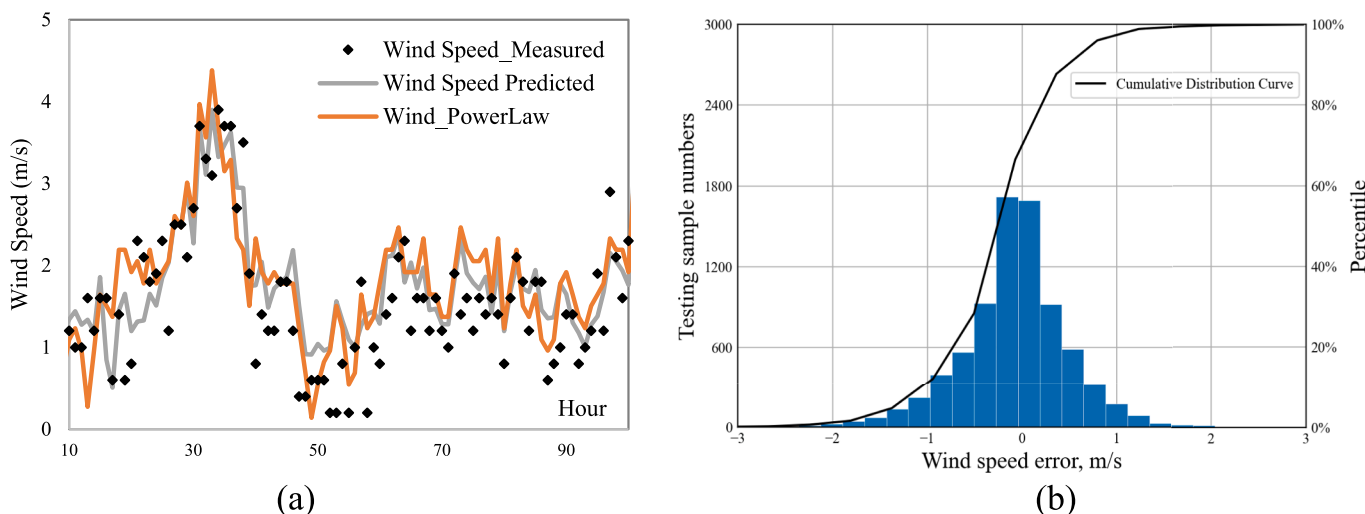


Fig. 6. (a) Wind speed comparison between measured, predicted, and calculated from power law distribution, (b) wind prediction error distribution for LOC1.

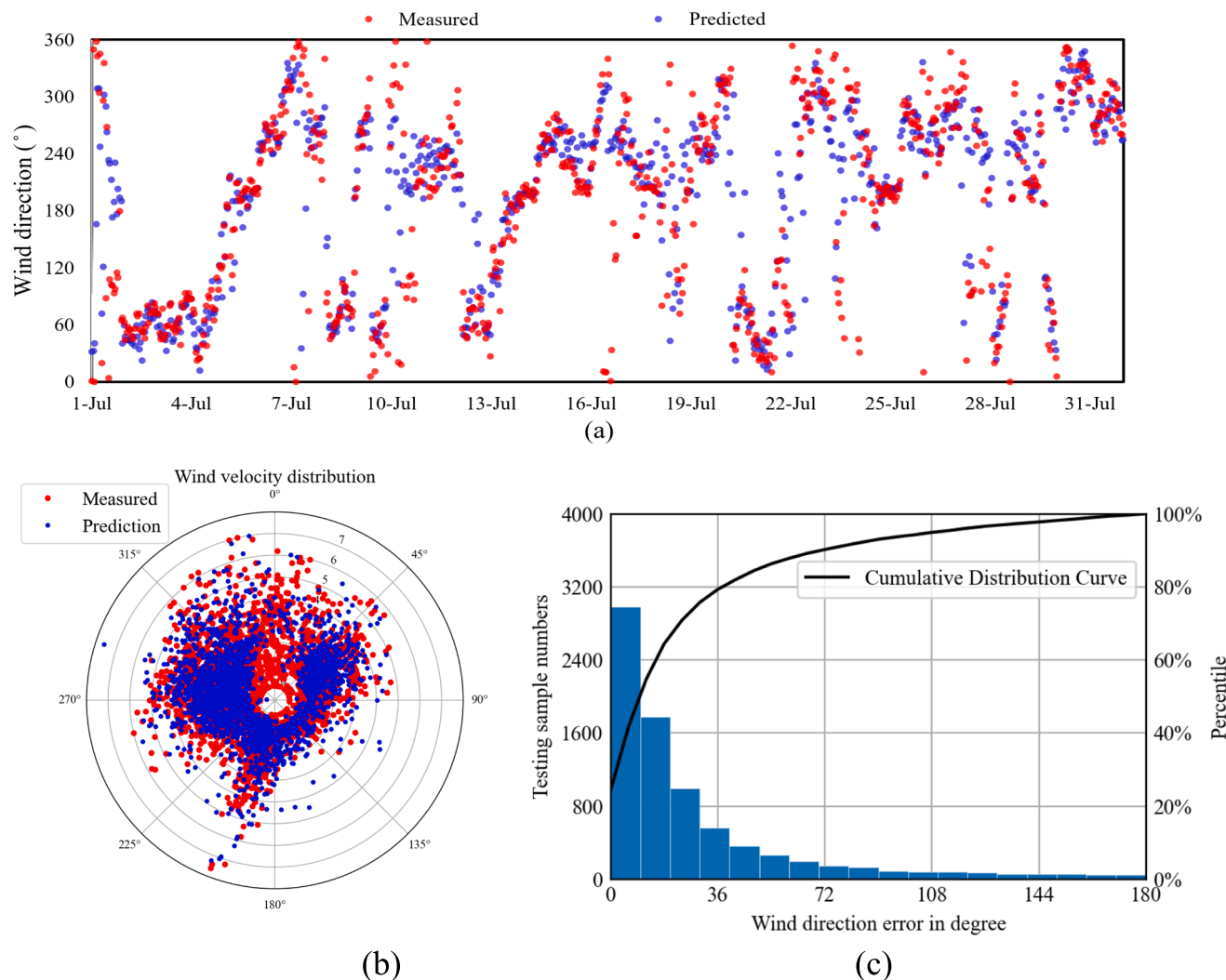


Fig. 7. (a) Temporal wind direction performance in July (b) Wind rose for testing dataset comparing the measured and predicted wind direction (c) Wind direction prediction error distribution for LOC1.

Table 4
Wind component and directions for 5 locations.

	MAE (degree)	RMSE (degree)	MAPE
LOC1	35	41	9.7 %
LOC2	30	35	8.3 %
LOC3	27	31	7.5 %
LOC4	31	38	8.6 %
LOC5	36	43	10.0 %

3.2. ANN applications – generation of local TMY and BEM analysis

3.2.1. Local TMYs

In urban microclimates, long-term weather can be predicted using projections from long-term historical weather data from airports with acceptable accuracy. The study collects historical weather records from 1997 to 2018 from the same location as the model training (Montréal-Trudeau International Airport). The TMY was calculated based on the weather at Trudeau International Airport for the past 20 years. The first step in obtaining the localized monthly data was to use historical weather station data for projections of local weather with our ANN-trained model in this study over the past 20 years. After projecting 20 years of microclimate data, the TMY algorithm will produce one-year weather conditions, i.e., local TMY with microclimate information

embedded, based on the past 20 years.

A comparison is shown in Fig. 8(a) between the traditional TMY results from the airport and the generated local TMY of LOC1. The local temperature from the airport can be up to 8 °C after the TMY algorithm at the airport from July 18th to July 23rd. It was found that urban microclimates under the TMY are different from the temperature at the airport (TMY_Airport), which causes traditional methods to underestimate urban outdoor thermal comfort and building energy consumption. A comparison of wind velocity between airport TMY and local TMY is shown in Fig. 8(b). Based on the TMY scale, there is a significant discrepancy between the wind speed at the airport and the local region (scaled on the same elevation by power law). As a result, when evaluating the overall building energy consumption, the wind pressure and CHTC around the building facade can be affected. We did not compare wind direction since the TMY method selects wind based on different years, and the variation of wind direction may not make the wind direction consistent in the two TMY methods.

3.2.2. BEM analysis

In this study, EnergyPlus evaluates building energy consumption based on the local TMY from 20 years of weather predictions for five individual locations. In Fig. 9, we present 20 years of weather predictions (e.g., TMY_LOC1) and baseline TMYs (TMY_BL) calculated from 20 years of airport weather. In addition, the figure presents an

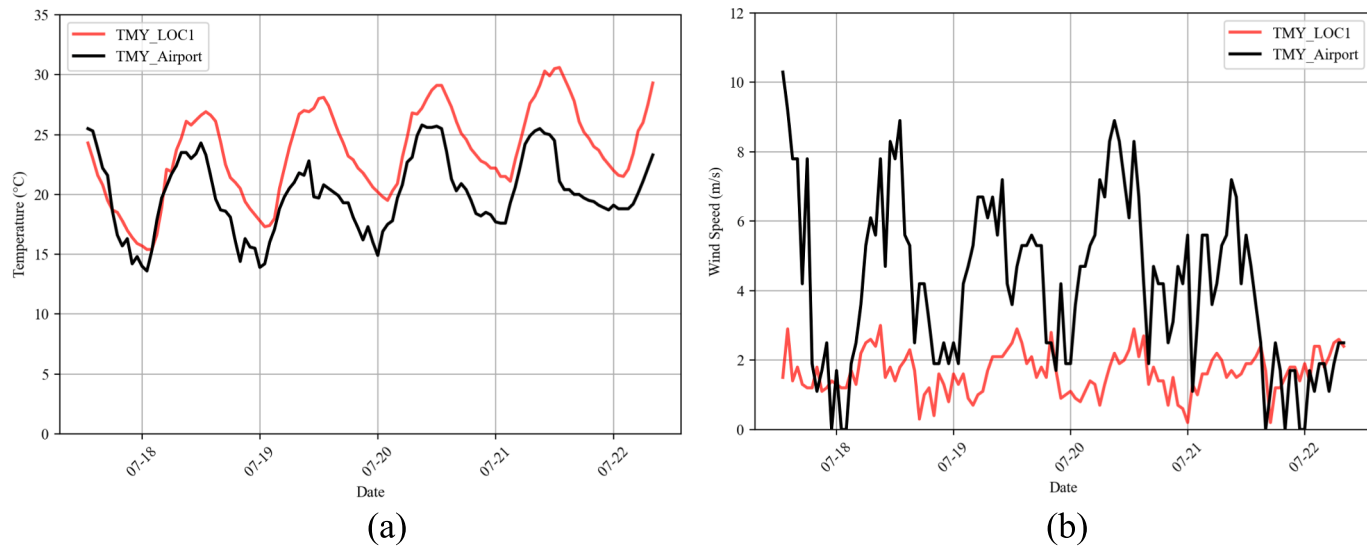


Fig. 8. TMY air temperature (a) and wind speed (b) at LOC1 from July 18th to 23rd.

evaluation of the cooling and heating loads on an annual basis. There appears to be a trend in the color band between the 20-year airport temperature and the 20-year local prediction temperature for four locations: LOC1, LOC2, LOC3, and LOC5. However, LOC4, which is located near a mountain park at high elevation, is less affected by urban microclimate than other locations. For LOC4, there is a full overlap between the 20 years of airport air temperature distribution and predicted local temperature. This indicates that the urban microclimate has the least impact at LOC4 than other locations.

In each month's analysis of heating and cooling energy, it is determined that 4 of 5 locations affected by urban microclimate will consume more cooling energy in the summer and less heat energy in the winter due to the higher ambient temperature caused by urban heat islands. Different seasons are affected differently by the urban heat island or urban microclimate. The energy consumption for LOC 1–5 has less impact on building energy in spring and fall, when there is less need for cooling or heating. The urban microclimate can have a significant effect on cooling energy, especially in June and July. However, for LOC4, where the ambient temperature differs less from the airport baseline, energy consumption is also close to the airport baseline, and urban microclimate impact becomes minimal compared to other locations.

Based on TMY weather from the airport, Fig. 10 illustrates an increase in cooling and a decrease in heating energy consumption. In this case study, the urban microclimate reduced winter heating energy consumption by 1 % to 10 %. Furthermore, it also increases cooling energy consumption by 2 % to 14 %. This not only shows that urban microclimate significantly impacts energy consumption [19], but also indicates that inside the same city, the spatial difference can also be great.

As a result of the spatial distribution of microclimate effects in Montreal, there is a noticeable spatial variation in energy consumption across locations. Urban heat islands have a lesser impact in places like LOC4, which are situated near mountains and parks. On the other hand, LOC3, located in densely populated areas, is more profoundly affected by the urban microclimate within a proximity of less than 5 km. Consequently, cooling energy consumption at LOC3 has increased by 11 %.

In light of this observation, it is important to consider the impact of urban microclimate on energy consumption. It suggests that energy consumption patterns in cities can vary significantly based on their specific location. Using such insights, urban planners and policymakers can optimize energy efficiency and mitigate energy consumption in different parts of cities.

3.3. Meteorological sensitivity analysis

The urban microclimate impact is determined by air temperature and wind in this study. To evaluate how air temperature, wind, and other meteorological parameters influence the building energy consumption values, we conducted a sensitivity analysis using the generated TMY weather data for LOC1 to investigate the relationship between meteorological parameters and building energy consumption. A detailed analysis of the results can be found in Appendix D. A Sensitivity Variance Index (SVI) was calculated to evaluate the influence of seven distinct meteorological parameters. The parameter with the highest impact received a rank of 1. The cooling load, heating load, and total load are exhaustively examined. Every section focuses on a specific parameter and its associated metrics. The parameters under consideration are air temperature, wind speed, wind direction, relative humidity (RH), global solar radiation, diffuse solar radiation, and normal solar radiation. A table presents key metrics for each parameter, including the Statistical Relevance Coefficient (SRC), Random Forest importance, T-value, and SVI. The metrics are accompanied by their respective rankings. Fig. 10 (b) illustrates the impact ranking based on the value in Appendix D. For both cooling and heating, the ambient air temperature is the most important parameter.

Air temperature is the most significant parameter in the cooling load section, with an SRC value of 0.72 and a top ranking of 1. There is a strong and statistically significant correlation between air temperature and cooling load, thus making it an essential factor to consider when analyzing cooling loads. In addition to its significance in predicting cooling load variations, Random Forest has an importance value of 308.94 for air temperature.

SVI values for wind speed and wind direction, however, are lower than those for other parameters, suggesting that they have a weaker correlation with cooling load. The results indicate that they have a relatively low impact, receiving ranks 4 and 6, respectively. The wind speed can have an impact on the building's ventilation energy cost, and wind direction has a limited impact on building energy modeling results. The relative humidity can have a high impact on building cooling in the summer, which can be further investigated if the study focuses on energy consumption during the summer. Solar radiation can also have an impact on energy consumption, however in the study, the local urban microclimate monitoring is on the roof and there is no shading impact information collected, solar radiation is considered not to vary with regions. If the specific building is located in a dense urban area, the solar radiation and shading should be considered carefully.

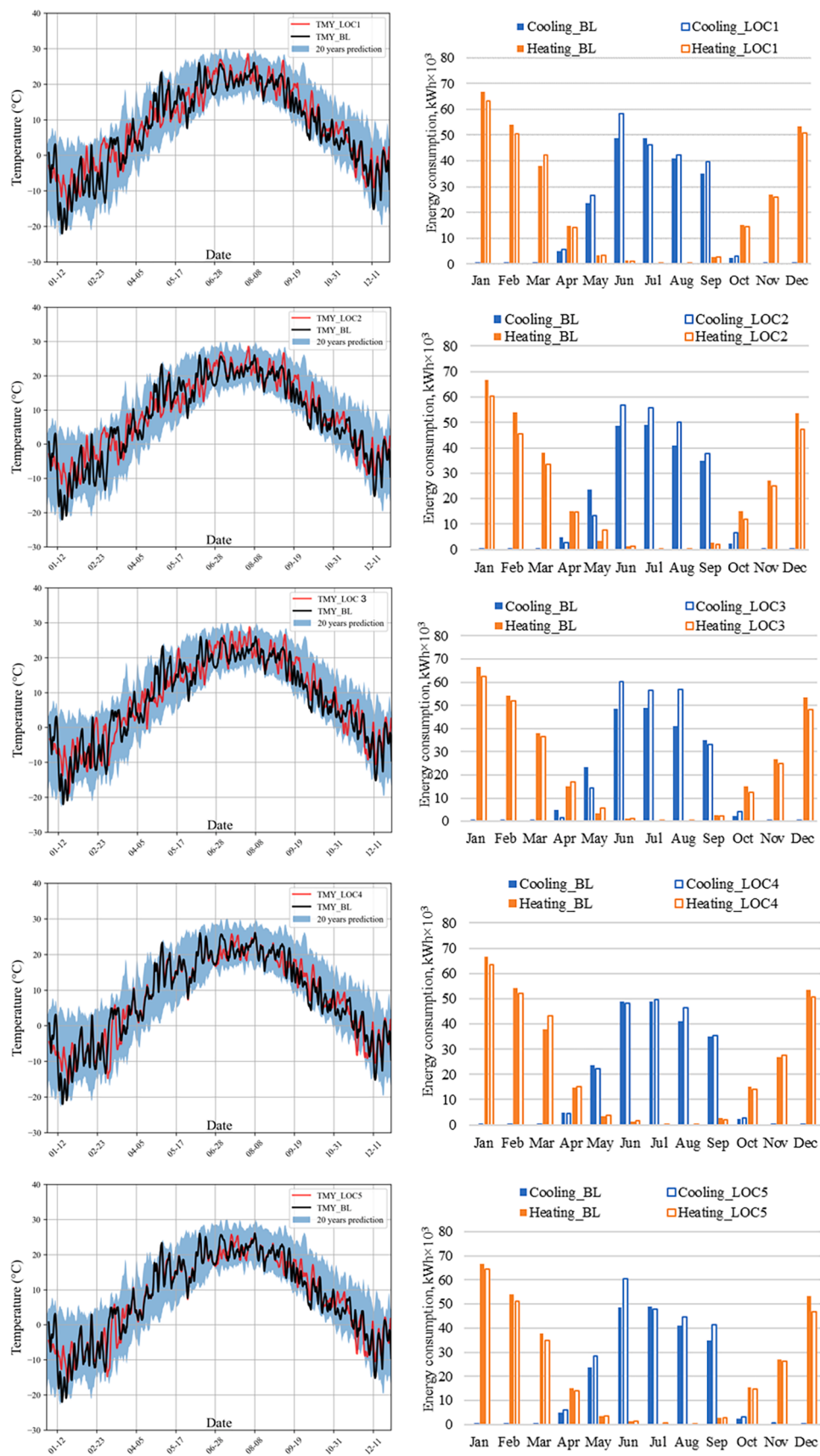


Fig. 9. Local 20 years weather prediction air temperature variation and related TMY and related annual cooling load and heating load evaluation for 5 Locations (LOC 1–5).

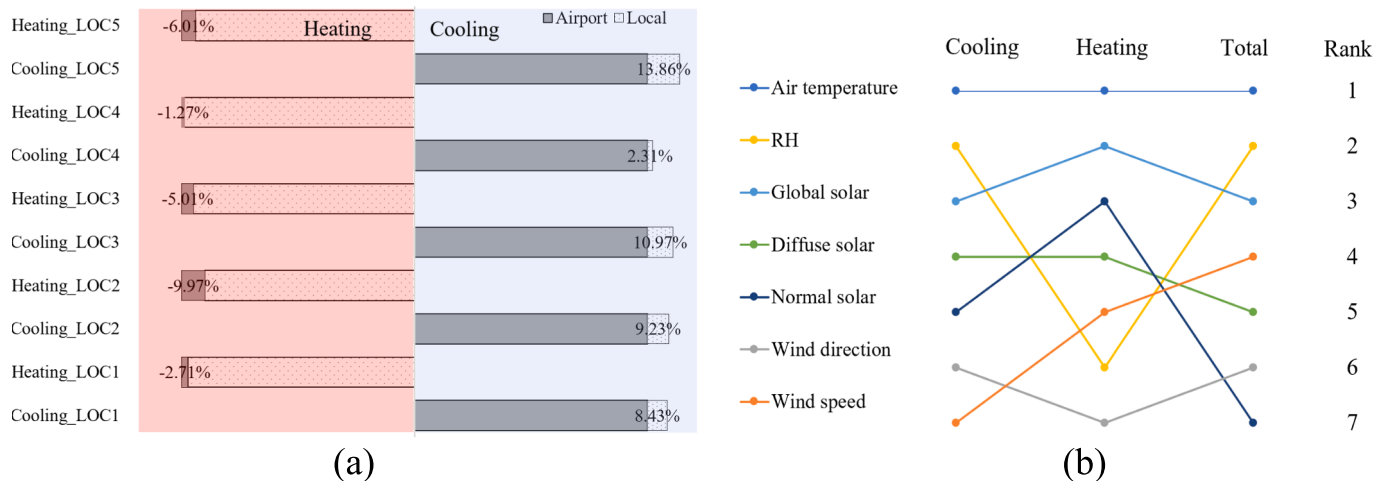


Fig. 10. (a) Overall cooling energy and heating energy changes in comparison to the traditional method using airport weather for TMY. (b) Meteorological parameters impact ranking on building energy modeling for LOC1.

Since the SVIs of other parameters are much lower than the SVIs of air temperature, their impact can be neglected compared to that of air temperature in all three load scenarios [59]. Except for temperature and wind, the other parameters are not discussed further in this study. However, further investigation of relative humidity and solar radiation remains to be done in the future.

4. Conclusions

Urban microclimate plays a significant role in the energy consumption of buildings. Accurate prediction of local weather conditions near a target building is crucial for estimating energy consumption under urban microclimate conditions. This study introduces a novel approach using an artificial neural network model to predict microclimate parameters based on long-term onsite measurements, highlighting its importance in building energy analysis.

The primary objective of this study is to establish a connection between urban microclimate parameters and public meteorological weather stations. The study presents the performance of the proposed model and methodology. Statistical investigations are conducted to compare the energy consumption for building heating and cooling against reference models using TMY weather data from the airport and localized weather conditions. Additionally, the study explores the spatial differences among different local weather stations in the urban microclimate's impact on building energy consumption. The findings of this study reveal that the urban microclimate can contribute to an additional 2 % to 14 % of building energy consumption across different locations.

Furthermore, the study reveals that air temperature holds the most importance in building energy modeling under urban microclimate. The level of relative humidity can significantly influence the cooling of buildings in the summer. Another factor affecting energy consumption is solar radiation. Consequently, solar radiation is assumed to be consistent across regions. Nevertheless, when dealing with buildings situated in densely populated urban areas, it is essential to give thorough consideration to solar radiation and shading effects. Wind speed and direction, which may affect building ventilation, play a lesser role compared to ambient air temperature in Montreal's climate conditions. Please note that their roles could be different in other climates. However, a similar analysis using the proposed method in this paper can be applied. Parameters including relative humidity and radiation are worth further investigation in future studies.

Overall, this study highlights the importance of accurate local weather prediction and its influence on building energy consumption

under urban microclimate conditions. The investigation of spatial differences among various local weather stations contributes to a comprehensive understanding of the urban microclimate's impact on building energy consumption.

4.1. Limitations and future work

Although this study provides valuable insights, certain limitations can be addressed to enhance future work. First, since the local weather stations in this study are installed on top of roofs, no shading effect has been observed at the measurement points. In fact, a weather station is often required to be installed at a location without shading so the proposed method was not designed to study the shading impacts on building energy performance, which, however, could play a major role in reality. So, this study does not take into account shading effects, and the spatial difference in the building façade was also neglected as other studies using TMYs. For future work, shading from surroundings, building shapes, and local urban morphology can be included, when these data are available. By incorporating these variables into the proposed model, a more detailed analysis of urban microclimate impacts can be evaluated for building energy performance. Additionally, the current model omits urban geometry as a feature. Microclimate conditions, such as wind patterns and heat distribution, are greatly influenced by urban form and layout. Considering urban geometry as a feature in future models would enhance the accuracy of predictions and enable a more holistic analysis of building energy consumption under different urban configurations. It is to be noted that the present study assumes that the microclimate model for urban areas will not change over time, which neglects the city's urban development. More dynamic weather data is needed to verify the model's time-invariance. In future models, adding the surrounding land use and land cover information could be a solution to consider urban development. Moreover, since the model must be trained separately for each location, the model cannot be generalized across different urban areas. In the future, more sophisticated models adding urban morphology indicators, including parameters such as sky view factor, average building height, openness, front area index, etc., as input features could be a potential solution, which can help create a more generalized model applicable to various urban contexts. In the future, more sophisticated models adding urban morphology indicators, including parameters such as sky view factor, average building height, openness, front area index, etc., as input features could be a potential solution, which can help create a more generalized model applicable to various urban contexts.

CRediT authorship contribution statement

Senwen Yang: Writing – review & editing, Writing – original draft, Visualization, Methodology, Investigation, Software, Formal analysis, Data curation, Conceptualization. **Dongxue Zhan:** Writing – review & editing, Visualization, Investigation, Formal analysis, Data curation. **Theodore Stathopoulos:** Formal analysis, Resources, Writing – original draft, Writing – review & editing, Supervision. **Jiwei Zou:** Writing – review & editing, Investigation, Data curation. **Chang Shu:** Writing – review & editing, Data curation. **Liangzhu Leon Wang:** Conceptualization, Formal analysis, Resources, Writing – original draft, Writing – review & editing, Supervision, Project administration, Funding acquisition.

Declaration of competing interest

The authors declare that they have no known competing financial

Appendix A

EnergyPlus simulation setup for building energy consumption simulation

Features	Description
Location	Montreal, Quebec, Canada
Building type	Commercial building
Number of Floors	1 story
Gross Floor Area	6871(m ²)/73,959 (ft ²)
HVAC system	VAV
Floor-to-Ceiling height	4
Window-to-wall ratio	35 %
Number of zones	25
Roof U-factor (W/(M ² K))	0.18
External Wall U-factor (W/(M ² K))	0.31
Window U-factor (W/(M ² K))	2.65
SHGC	0.43
Infiltration	1.5 cfm/ft ²
Heating setpoint	6:00–21:00 21 °C Others 16 °C
Cooling setpoint	6:00–21:00 24 °C Others 27 °C
People density	Classroom: 4 m ² /person Corridor: 10 m ² /person Office: 20 m ² /person Gym: 3.33 m ² /person Kitchen: 25.2 m ² /person Cafeteria: 1.39 m ² /person Library: 4.35 m ² /person Classroom: 0.008 (m ³ /s)/person Library media center: 0.008 (m ³ /s)/person Office: 0.01 (m ³ /s)/person Gym: 0.01 (m ³ /s)/person Kitchen: 0.008 (m ³ /s)/person Cafeteria: 0.01 (m ³ /s)/person Corridor: 0.0005 (m ³ /s)/m ²
Ventilation rate	

interests or personal relationships that could have appeared to influence the work reported in this paper.

Data availability

Data will be made available on request.

Acknowledgment

The research is supported by the Natural Sciences and Engineering Research Council (NSERC) of Canada through the Discovery Grants Program [#RGPIN-2018-06734] and the Advancing Climate Change Science in Canada Program [#ACCPJ 535986-18].

Appendix B

Weather station

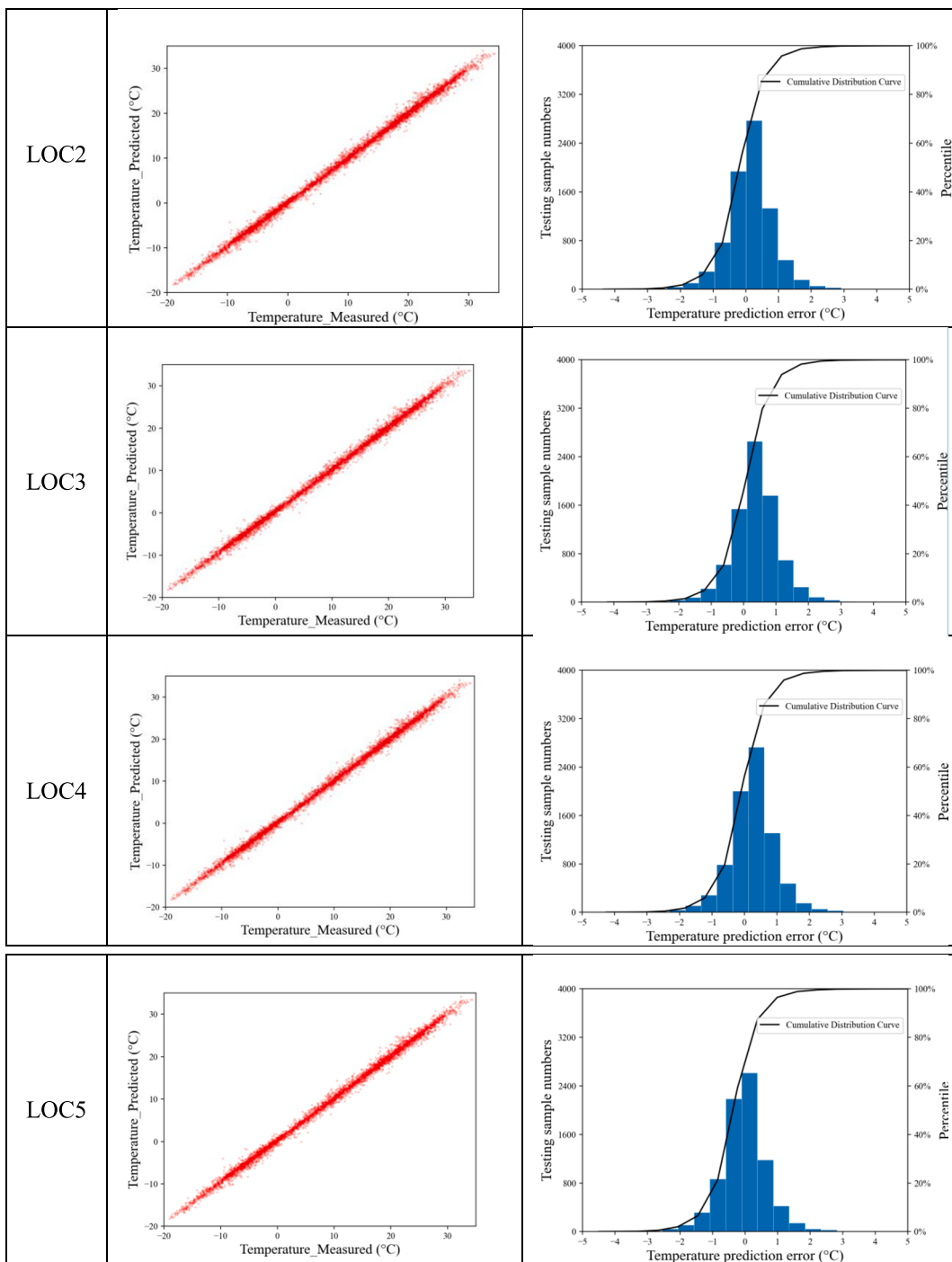
Location	Installation	Elevation	Roughness exponent (Power Law)
LOC 1		18 m	0.25
LOC 2		16 m	0.35
LOC 3		23 m	0.35
LOC 4		30 m	0.35
LOC 5		13 m	0.3

Weather station sensors and their parameters

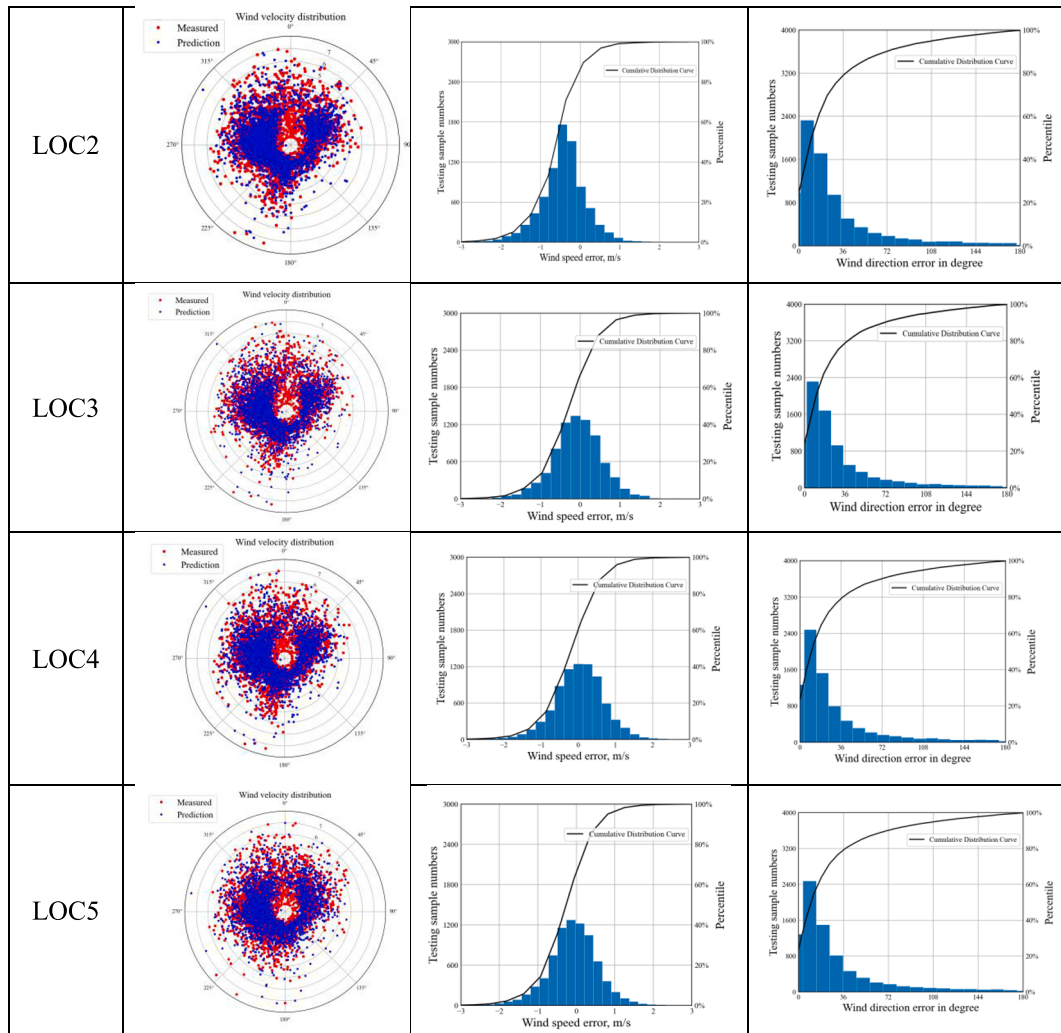
Type	Temperature sensor	Wind speed sensor	Wind direction sensor
Model	S-THB-M002	RM Young	RM Young
Range	-40 °C – 75 °C	0–76 m/s	0–355°, 5° dead band
Accuracy	±0.21 °C; 0° – 50 °C	±1.1 m/sec or ± 4 %	±5°
Resolution	0.02 °C at 25 °C	0.2 m/s	1.4°
Operation Condition	-40 °C – 75 °C	-40° – 75 °C	-40 °C – 70 °C
Response Time	5 min	N/a	N/a

Appendix C

Temperature prediction for LOC 2–5.



Wind speed and direction prediction for LOC 2–5.



Appendix D

Results of meteorological parameters' sensitivity analysis.

For cooling load					
Parameter	SRC	Random forest	T-value	SVI	Rank
Air temperature	0.72	308.94	64.05	54.05	1
Wind speed	0.05	18.09	4.93	3.64	7
Wind direction	0.05	22.6	4.71	3.82	6
RH	0.13	119.4	12.58	14.33	2
Global Solar	0.31	11.37	11.04	10.3	3
Diffuse Solar	0.19	10.26	10.89	7.75	4
Normal Solar	0.16	11.21	7.22	6.11	5
For heating load					
Parameter	SRC	Random forest	T-value	SVI	Rank
Air temperature	0.7	406.46	56.93	60.98	1
Wind speed	0.05	29.34	4.17	4.28	5
Wind direction	0	42.73	0.27	2.5	7
RH	0.01	53.57	1.11	3.66	6
Global Solar	0.19	52.9	6.4	10.07	2
Diffuse Solar	0.19	13.94	9.96	9.16	4
Normal solar	0.21	12.9	8.96	9.34	3
For total load					
Parameter	SRC	Random forest	T-value	SVI	Rank
Air temperature	0.38	271.7	25.53	42.55	1
Wind speed	0.08	37.82	5.94	8.14	4
Wind direction	0.05	47.95	3.7	6.39	6
RH	0.13	140.47	9.69	17.91	2
Global Solar	0.22	48.21	5.98	13.43	3
Diffuse solar	0.1	20.51	4.21	6.79	5
Normal solar	0.05	39.32	1.7	4.79	7

References

- [1] L. Ji, A. Laouadi, C. Shu, A. Gaur, M. Lacasse, L. (Leon) Wang, Evaluating approaches of selecting extreme hot years for assessing building overheating conditions during heatwaves, Energy Build. (2022), <https://doi.org/10.1016/j.enbuild.2021.111610>.
- [2] C. Shu, A. Gaur, L. Wang, M.A. Lacasse, Evolution of the local climate in Montreal and Ottawa before, during and after a heatwave and the effects on urban heat islands, Sci. Total Environ. (2023), <https://doi.org/10.1016/j.scitotenv.2023.164497>.
- [3] L.H.U.W. Abeydeera, J.W. Mesthrige, T.I. Samarasinghalage, Global research on carbon emissions: A scientometric review, Sustain. (2019), <https://doi.org/10.3390/su11143972>.
- [4] H. Bherwani, A. Singh, R. Kumar, Assessment methods of urban microclimate and its parameters: A critical review to take the research from lab to land, Urban Clim. (2020), <https://doi.org/10.1016/j.uclim.2020.100690>.
- [5] Z. Zeng, X. Zhou, L. Li, The Impact of Water on Microclimate in Lingnan Area, Procedia Eng. (2017), <https://doi.org/10.1016/j.proeng.2017.10.082>.
- [6] S. Yang, L. (Leon) Wang, T. Stathopoulos, A.M. Marey, Urban microclimate and its impact on built environment – A review, Build. Environ. 238 (2023) 110334. <https://doi.org/10.1016/j.buildenv.2023.110334>.
- [7] L.P. Muniz-Gäal, C.C. Pezzuto, M.F.H. de Carvalho, L.T.M. Mota, Urban geometry and the microclimate of street canyons in tropical climate, Build. Environ. (2020), <https://doi.org/10.1016/j.buildenv.2019.106547>.
- [8] A. Shafaghat, G. Manteghi, A. Keyvanfar, H. Bin Lamit, K. Saito, D.R. Ossen, Street geometry factors influence urban microclimate in tropical coastal cities: A review, Environ. Clim. Technol. (2016), <https://doi.org/10.1515/rteuct-2016-0006>.
- [9] A.S. Jihad, M. Tahiri, Modeling the urban geometry influence on outdoor thermal comfort in the case of Moroccan microclimate, Urban Clim. (2016), <https://doi.org/10.1016/j.uclim.2016.02.002>.
- [10] A. Aboelata, Vegetation in different street orientations of aspect ratio (H/W 1:1) to mitigate UHI and reduce buildings' energy in arid climate, Build. Environ. (2020), <https://doi.org/10.1016/j.buildenv.2020.106712>.
- [11] A. Katal, S. Leroyer, J. Zou, O. Nikiema, M. Albettar, S. Belair, L. (Leon) Wang, Outdoor heat stress assessment using an integrated multi-scale numerical weather prediction system: A case study of a heatwave in Montreal, Sci. Total Environ. (2023), <https://doi.org/10.1016/j.scitotenv.2022.161276>.
- [12] H. Ji, Y. Peng, W. Ding, A quantitative study of geometric characteristics of urban space based on the correlation with microclimate, Sustain. (2019), <https://doi.org/10.3390/su11184951>.
- [13] L. Tian, Y. Li, J. Lu, J. Wang, Review on urban heat island in china: Methods, its impact on buildings energy demand and mitigation strategies, Sustain. (2021), <https://doi.org/10.3390/su13020762>.
- [14] A. Salvati, H. Coch Roura, C. Cecere, Assessing the urban heat island and its energy impact on residential buildings in Mediterranean climate: Barcelona case study, Energy Build. (2017), <https://doi.org/10.1016/j.enbuild.2017.04.025>.
- [15] P. Coseo, L. Larsen, How factors of land use/land cover, building configuration, and adjacent heat sources and sinks explain Urban Heat Islands in Chicago, Landsc. Urban Plan. (2014), <https://doi.org/10.1016/j.landurbplan.2014.02.019>.
- [16] T. Hong, Y. Xu, K. Sun, W. Zhang, X. Luo, B. Hooper, Urban microclimate and its impact on building performance: A case study of San Francisco, Urban Clim. (2021), <https://doi.org/10.1016/j.uclim.2021.100871>.
- [17] K. Lundgren, T. Kjellstrom, Sustainability challenges from climate change and air conditioning use in urban areas, Sustain. (2013), <https://doi.org/10.3390/su5073116>.
- [18] J. Allegritti, V. Dorer, J. Carmeliet, Coupled CFD, radiation and building energy model for studying heat fluxes in an urban environment with generic building configurations, Sustain. Cities Soc. (2015), <https://doi.org/10.1016/j.scs.2015.07.009>.
- [19] X. Li, Y. Zhou, S. Yu, G. Jia, H. Li, W. Li, Urban heat island impacts on building energy consumption: A review of approaches and findings, Energy (2019), <https://doi.org/10.1016/j.energy.2019.02.183>.
- [20] J. Liu, M. Heidarinejad, S.K. Nikkho, N.W. Mattise, J. Srebric, Quantifying impacts of urban microclimate on a building energy consumption-a case study, Sustain. (2019), <https://doi.org/10.3390/su11184921>.
- [21] M. Palme, L. Inostroza, G. Villacreses, A. Lobato, C. Carrasco, Urban weather data and building models for the inclusion of the urban heat island effect in building performance simulation, Data Br. (2017), <https://doi.org/10.1016/j.dib.2017.08.035>.
- [22] N. Sezer, H. Yoonus, D. Zhan, L. (Leon) Wang, I.G. Hassan, M.A. Rahman, Urban microclimate and building energy models: A review of the latest progress in coupling strategies, Renew. Sustain. Energy Rev. (2023), <https://doi.org/10.1016/j.rser.2023.113577>.

- [23] N. Lauzet, A. Rodler, M. Musy, M.H. Azam, S. Guernouti, D. Mauree, T. Colinart, How building energy models take the local climate into account in an urban context – A review, Renew. Sustain. Energy Rev. (2019), <https://doi.org/10.1016/j.rser.2019.109390>.
- [24] N.H. Wong, Y. He, N.S. Nguyen, S.V. Raghavan, M. Martin, D.J.C. Hii, Z. Yu, J. Deng, An integrated multiscale urban microclimate model for the urban thermal environment, Urban Clim. (2021), <https://doi.org/10.1016/j.uclim.2020.100730>.
- [25] G. Xu, J. Li, Y. Shi, X. Feng, Y. Zhang, Improvements, extensions, and validation of the Urban Weather Generator (UWG) for performance-oriented neighborhood planning, Urban Clim. (2022), <https://doi.org/10.1016/j.uclim.2022.101247>.
- [26] A. Salvati, M. Palme, L. Inostroza, Key parameters for urban heat island assessment in A Mediterranean context: A sensitivity analysis using the urban weather generator model, IOP Conf. Ser. Mater. Sci. Eng. (2017), <https://doi.org/10.1088/1757-899X/245/8/082055>.
- [27] A. Kamal, S.M.H. Abidi, A. Mahfouz, S. Kadam, A. Rahman, I.G. Hassan, L.L. Wang, Impact of urban morphology on urban microclimate and building energy loads, Energy Build. (2021), <https://doi.org/10.1016/j.enbuild.2021.111499>.
- [28] J. Pfafferott, S. Rißmann, M. Sühring, F. Kanani-Sühring, B. Maronga, Building indoor model in PALM-4U: Indoor climate, energy demand, and the interaction between buildings and the urban microclimate, Geosci. Model Dev. (2021), <https://doi.org/10.5194/gmd-14-3511-2021>.
- [29] J. Vogel, A. Afshari, G. Chockalingam, S. Stadler, Evaluation of a novel WRF/PALM-4U coupling scheme incorporating a roughness-corrected surface layer representation, Urban Clim. (2022), <https://doi.org/10.1016/j.uclim.2022.101311>.
- [30] J. Geletić, M. Lehner, P. Krč, J. Resler, E.S. Krayenhoff, High-resolution modelling of thermal exposure during a hot spell: A case study using palm-4u in prague, czech republic, Atmosphere (basel). (2021), <https://doi.org/10.3390/atmos12020175>.
- [31] M. Hadavi, H. Pasdarshahri, Impacts of urban buildings on microclimate and cooling systems efficiency: Coupled CFD and BES simulations, Sustain. Cities Soc. (2021), <https://doi.org/10.1016/j.jscs.2021.102740>.
- [32] S. Tsoka, K. Tolika, T. Theodosiou, K. Tsikaloudaki, D. Bikas, A method to account for the urban microclimate on the creation of ‘typical weather year’ datasets for building energy simulation, using stochastically generated data, Energy Build. (2018), <https://doi.org/10.1016/j.enbuild.2018.01.016>.
- [33] K. Häb, A. Middel, B.L. Ruddell, H. Hagen, A Data-Driven Approach to Categorize Climatic Microenvironments, in: EnvirVis 2016 - Work. Vis. Environ. Sci., 2016. <https://doi.org/10.2321/enviris.20161105>.
- [34] L. Alonso, F. Renard, A new approach for understanding urban microclimate by integrating complementary predictors at different scales in regression and machine learning models, Remote Sens. (2020), <https://doi.org/10.3390/RS12152434>.
- [35] G.Y. Oukawa, P. Krecl, A.C. Targino, Fine-scale modeling of the urban heat island: A comparison of multiple linear regression and random forest approaches, Sci. Total Environ. 815 (2022) 152836, <https://doi.org/10.1016/j.scitotenv.2021.152836>.
- [36] C. Ding, K.P. Lam, Data-driven model for cross ventilation potential in high-density cities based on coupled CFD simulation and machine learning, Build. Environ. (2019), <https://doi.org/10.1016/j.buldev.2019.106394>.
- [37] M. Mortezaeejad, J. Zou, M. Hosseini, S. Yang, L. Wang, Estimating urban wind speeds and wind power potentials based on machine learning with city fast fluid dynamics training data, Atmosphere (Basel) (2022), <https://doi.org/10.3390/atmos13020214>.
- [38] M. Zhang, X. Zhang, S. Guo, X. Xu, J. Chen, W. Wang, Urban micro-climate prediction through long short-term memory network with long-term monitoring for on-site building energy estimation, Sustain. Cities Soc. (2021), <https://doi.org/10.1016/j.jscs.2021.103227>.
- [39] S. Moghanlo, M. Alavinejad, V. Oskoei, H. Najafi Saleh, A.A. Mohammadi, H. Mohammadi, Z. DerakhshanNejad, Using artificial neural networks to model the impacts of climate change on dust phenomenon in the Zanjan region, north-west Iran, Urban Clim. (2021), <https://doi.org/10.1016/j.uclim.2020.100750>.
- [40] Y. Xie, W. Hu, X. Zhou, S. Yan, C. Li, Artificial neural network modeling for predicting and evaluating the mean radiant temperature around buildings on hot summer days, Buildings (2022), <https://doi.org/10.3390/buildings12050513>.
- [41] D. Guijo-Rubio, A.M. Durán-Rosal, P.A. Gutiérrez, A.M. Gómez-Orellana, C. Casanova-Mateo, J. Sanz-Justo, S. Salcedo-Sanz, C. Hervás-Martínez, Evolutionary artificial neural networks for accurate solar radiation prediction, Energy (2020), <https://doi.org/10.1016/j.energy.2020.118374>.
- [42] B. Shboul, I. AL-Arfi, S. Michailos, D. Ingham, L. Ma, K.J. Hughes, M. Pourkashanian, A new ANN model for hourly solar radiation and wind speed prediction: A case study over the north & south of the Arabian Peninsula, Sustain. Energy Technol. Assessments (2021), <https://doi.org/10.1016/j.seta.2021.101248>.
- [43] J. Zou, A. Gaur, L. (Leon) Wang, A. Laouadi, M. Lacasse, Assessment of future overheating conditions in Canadian cities using a reference year selection method, Build. Environ. (2022), <https://doi.org/10.1016/j.buldev.2022.109102>.
- [44] D.B. Crawley, L.K. Lawrie, F.C. Winkelmann, W.F. Buhl, Y.J. Huang, C.O. Pedersen, R.K. Strand, R.J. Liesen, D.E. Fisher, M.J. Witte, J. Glazer, EnergyPlus: creating a new-generation building energy simulation program, Energy Build. 33 (2001) 319–331, [https://doi.org/10.1016/S0378-7788\(00\)00114-6](https://doi.org/10.1016/S0378-7788(00)00114-6).
- [45] C.Y. Siu, Z. Liao, Is building energy simulation based on TMY representative: A comparative simulation study on doe reference buildings in Toronto with typical year and historical year type weather files, Energy Build. (2020), <https://doi.org/10.1016/j.enbuild.2020.109760>.
- [46] J. Zhang, F. Zhang, Z. Gou, J. Liu, Assessment of macroclimate and microclimate effects on outdoor thermal comfort via artificial neural network models, Urban Clim. (2022), <https://doi.org/10.1016/j.uclim.2022.101134>.
- [47] X. Wu, J. Hou, J. Hui, Z. Tang, W. Wang, Revealing Microclimate around Buildings with Long-Term Monitoring through the Neural Network Algorithms, Buildings. (2022), <https://doi.org/10.3390/buildings12040395>.
- [48] S. Higgins, T. Stathopoulos, Application of artificial intelligence to urban wind energy, Build. Environ. (2021), <https://doi.org/10.1016/j.buldev.2021.107848>.
- [49] J. Zou, H. Lu, C. Shu, L. Ji, A. Gaur, L. (Leon) Wang, Multiscale numerical assessment of urban overheating under climate projections: A review, Urban Clim. 49 (2023) 101551, <https://doi.org/10.1016/j.uclim.2023.101551>.
- [50] M.P. Tootkaboni, I. Ballarini, M. Zinzi, V. Corrado, A comparative analysis of different future weather data for building energy performance simulation, Climate (2021), <https://doi.org/10.3390/cl9020037>.
- [51] C. Zhang, O.B. Kazanci, S. Attia, R. Levinson, B.W.O. Sang Hoon Lee, Peter Holzer, Agnieszka Salvat, Anaïs Machard, Mamak Pourabdollahtootkaboni, Abhishek Gaur, General rights IEA EBC Annex 80-Dynamic simulation guideline for the performance testing of resilient cooling strategies, Citation. (2021).
- [52] M. Deru, K. Field, D. Studer, K. Benne, B. Griffith, P. Torcellini, B. Liu, M. Halverson, D. Winiarski, M. Rosenberg, M. Yazdanian, J. Huang, D. Crawley, U. S. Department of Energy commercial reference building models of the national building stock, Publ. (2011) 1–118. http://digitalscholarship.unlv.edu/renew_pubs/44.
- [53] K. Menberg, Y. Heo, R. Choudhary, Sensitivity analysis methods for building energy models: Comparing computational costs and extractable information, Energy Build. (2016), <https://doi.org/10.1016/j.enbuild.2016.10.005>.
- [54] T. Wei, A review of sensitivity analysis methods in building energy analysis, Renew. Sustain. Energy Rev. (2013), <https://doi.org/10.1016/j.rser.2012.12.014>.
- [55] H. Lim, Z.J. Zhai, Comprehensive evaluation of the influence of meta-models on Bayesian calibration, Energy Build. (2017), <https://doi.org/10.1016/j.enbuild.2017.09.009>.
- [56] C. Shu, Assessment of the Effects of Extreme Heat Events on Buildings, Concordia Univ. 2021. PhD thesis.
- [57] E.W. Peterson, J.P. Hennessey, On the use of power laws for estimates of wind power potential, J. Appl. Meteorol. (1978), [https://doi.org/10.1175/1520-0450\(1978\)017<0390:OTUOPL>2.0.CO;2](https://doi.org/10.1175/1520-0450(1978)017<0390:OTUOPL>2.0.CO;2).
- [58] S. Magli, C. Lodi, L. Lombroso, A. Muscio, S. Teggi, Analysis of the urban heat island effects on building energy consumption, Int. J. Energy Environ. Eng. (2015), <https://doi.org/10.1007/s40095-014-0154-9>.
- [59] D. Hou, I.G. Hassan, L. Wang, Review on building energy model calibration by Bayesian inference, Renew. Sustain. Energy Rev. (2021), <https://doi.org/10.1016/j.rser.2021.110930>.